Journal Name

ARTICLE TYPE

Cite this: DOI: 00.0000/xxxxxxxxxx

Nature of hydrated proton vibrations revealed by nonlinear spectroscopy of acid water nanodroplets†

Oleksandr O. Sofronov[a] and Huib J. Bakker*[a]

Received Date
Accepted Date

DOI: 00.0000/xxxxxxxxxx

We use polarization-resolved femtosecond pump-probe spectroscopy to investigate the vibrations of hydrated protons in anionic (AOT) and cationic (CTAB/hexanol) reverse micelles in the frequency range 2000-3500 cm^{-1}. For small AOT micelles the dominant proton hydration structure consists of H_3O^+ with two OH groups donating hydrogen bonds to water molecules, and one OH group donating a weaker hydrogen bond to sulfonate. For cationic reverse micelles, we find that the absorption at frequencies >2500 cm^{-1} is dominated by asymmetric proton-hydration structures in which one of the OH groups of H_3O^+ is more weakly hydrogen-bond to water than the other two OH groups.

In aqueous solution, the proton (H^+) exists in the form of extended dynamic hydration structures. These hydration structures rapidly interconvert, thus facilitating fast diffusion of the proton charge.[1–3] Multiple experimental and theoretical studies conclude that the preferential proton hydration structure is a distorted $H_3O^+(H_2O)_3$ Eigen[2–5] or $H_5O_2^+$ Zundel[6–9] cation, or an intermediate structure showing both Eigen and Zundel character[10–14]. Which of these hydration structures is predominantly present in aqueous media, is still under debate.

To obtain the pure spectrum of the hydrated proton in aqueous solution one would have to subtract the spectral response of water molecules that are not participating in proton hydration. Unfortunately, it is not possible to determine the absorption spectrum of the hydrated proton without any ambiguity because the fraction of water molecules that is not affected by proton charge is not precisely known. By subtracting the maximum possible amplitude of the water spectrum without the appearance of negative signals, we obtain the infrared spectrum shown in Fig. 1A, that forms an approximation of the infrared spectrum of the hydrated proton.

The infrared absorption spectrum of the hydrated proton in aqueous solution (black line in Fig. 1A) shows a broad absorption continuum at frequencies <3000 cm^{-1}. Most of the studies assign the high frequency part (>2000 cm^{-1}) of this continuum to the OH-stretch vibrations of the hydrated proton, the band centered at $\sim$1750 cm^{-1} to the bending vibrations of the hydrated proton, and the broad band at 1200 cm^{-1} to the proton transfer mode – i.e. the shuttling vibration of the central proton in a Zundel-type $H_5O_2^+$ configuration.[4,7,14,15]

The OH-stretch absorption appears as a nearly flat signal in the frequency range of 2000-2500 cm^{-1} and a broad band at higher frequency with a maximum at $\sim$3000 cm^{-1}. Studies of small protonated water clusters show that the OH-stretch vibrations of strongly hydrogen bonded OH-groups are shifted to lower frequencies with respect to the OH stretch vibrations of water molecules.[16–18] When the positive charge resides on a hydrogen atom, the corresponding OH-group becomes more polar, which increases the hydrogen-bond interaction and leads to a shift of the OH-stretch vibration to lower frequency. Hence, one of the possible interpretations of the extremely broad OH-stretch spectrum of hydrated protons is that this spectrum results from the existence of a large variety of (transient) structures with different geometries and charge distributions.

Here we study the vibrational spectrum and the structure of hydrated protons in water nanodroplets of reverse micelles. Reverse micelles are widely used as nanoreactors for proton-mediated processes, such as acid catalyzed polymerization.[19–21] Besides this, reverse micelles have important advantages for a femtosecond infrared spectroscopic study of proton solvation in liquid water. First, they allow the preparation of samples with an overall low water concentration, which is useful in view of the strong absorption of the molecular vibrations of water. At the same time, the spectroscopic properties of water in nanodroplets are more similar to those in bulk water, than the properties of isolated water molecules or small water clusters. Second, the nonpolar solvent, which forms the continuous phase of the microemulsion,

[a] AMOLF, Science Park 104, 1098 XG Amsterdam, The Netherlands. Tel: + 31 20 7547128; E-mail: h.bakker@amolf.nl

† Electronic Supplementary Information (ESI) available: Experimental details; determination of the size of the nanodroplets; delay time dependence of the transient spectra for protons in AOT reverse micelles; infrared spectra of concentrated solutions of ethanesulfonic acid. See DOI: 00.0000/00000000.

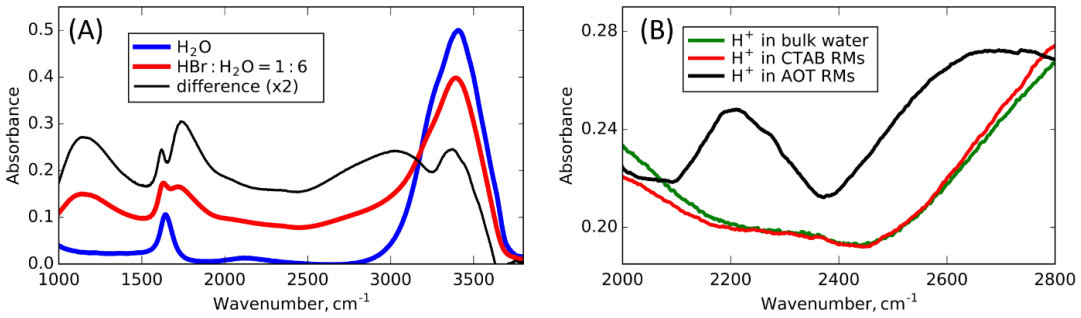

Fig. 1 (A) Fourier-transform infrared spectra of neat water (blue), HBr solution (red) and their weighted difference (black). (B) Zoomed in spectra of the hydrated proton in bulk aqueous solution (green) and in CTAB (red) and AOT (black) reverse micelles.

can act as a heat bath that accepts the energy dumped in the sample by exciting the water molecules in the reverse micelles with a laser pulse. This energy uptake by the nonpolar solvent reduces the signal contribution of the isotropic response of the heating of water. All these factors make reverse micelles a favorable system to study the vibrational spectrum of hydrated protons.

The drawback of reverse micelles as a model system to study the vibrational response of hydrated protons is that the solvation of chemical species and the dynamics of chemical processes can be different from bulk solutions. This difference can originate either from the special solvent properties of the confined water or from specific interactions with the molecular groups of the surfactant molecules located at the surface of the water nanodroplet.[22,23]

In Fig. 1B we show the linear infrared absorption spectrum of hydrated protons in anionic (AOT as surfactant) and cationic (CTAB as surfactant) reverse micelles, in the frequency range 2000-2800 cm^{-1}. The infrared spectrum of hydrated protons in cationic reverse micelles resembles closely the spectrum of hydrated protons in bulk water, probably because the protons are repelled by the positive charges of the surfactant, with the result that the protons reside predominantly in the bulk-like core of the water nanodroplet. For the anionic reverse micelles we observe a strong additional absorption band at ∼2200 cm^{-1}. Interestingly, the absorption spectrum of the cationic reverse micelles and bulk water also shows the presence of a weak absorption band at ∼2350 cm^{-1}. This band is not an artifact of the subtraction procedure. In fact, a strong band near this frequency has been observed by Fournier et al. in a two-dimensional infrared (2D-IR) spectroscopic study of aqueous HCl solutions.[8]

A highly suitable technique to study the structure and dynamics of hydrated protons in different environments is femtosecond nonlinear vibrational spectroscopy. This technique has been used to study the vibrational relaxation dynamics of the bending and OH-stretch vibrations of small protonated water clusters in polar solvents (acetonitrile[24–26] and dimethyl sulfoxide[27]). These studies showed that the vibrationally excited states of proton hydration structures relax with a time constant T_1 <100 fs, leading to ultrafast heating of the direct environment of the proton. The vibrational relaxation is followed by a slower process of in which the heat is redistributed over the solution.

Femtosecond nonlinear vibrational spectroscopy has also been used to study the OH-stretch vibrations of the asymmetric Zundel-cation in water, in particular to investigate the properties of the proton transfer mode.[7,8] It was shown that the experimental data can be well explained with an asymmetric quartic potential for this vibration. Fournier et al.[8] used polarization-resolved femtosecond nonlinear vibrational spectroscopy to study the orientation of hydrated proton bending modes with respect to the proton transfer mode and the OH-stretch modes. In another study[28] the anisotropy dynamics of the bending modes of the hydrated proton were measured, and used to estimate the proton transfer time in water. Recently, we used single-color polarization-resolved femtosecond nonlinear vibrational spectroscopy to study the OH-stretch vibrations of hydrated protons in nanoconfined aqueous environments[29] We observed that nanoconfinement leads to a strong slowing down of aqueous proton transfer.

Here we use two-color polarization-resolved femtosecond nonlinear vibrational spectroscopy infrared (fs-IR) pump-probe spectroscopy to investigate the structure-spectrum relation of the OH-stretch vibrations of proton solvation structures in liquid water. We perform these experiments for protons in reverse micelles (microemulsions), i.e. water nanodroplets in an apolar solvent that are stabilized by anionic (AOT) and cationic (CTAB/hexanol) surfactants.

In our pump-probe experiments we excite OH-stretch vibrations of the proton hydration structures with an intense mid-infrared pulse. The excited stretch vibrations of OH-groups that carry a significant amount of the proton charge relax on sub-100 fs time scale by transferring the vibrational energy to the adjacent hydrogen bonds.[24–26,28] This process results in a “locally hot state”, in which the hydrogen bonds in the local proton hydration structure are weakened due to the dumped energy, similarly to the effect of thermal heating. This non-equilibrium state typically persists for picoseconds before the excess energy is equilibrated over a bigger volume. The locally hot state has an absorption spectrum different from that of the hydrated protons in the equilibrium state. We measure this absorption change with a weaker probe pulse delayed in time.

In Fig. 2 we show the isotropic transient absorption spectra for hydrated protons in anionic (A) and cationic (B) reverse micelles of different size following the excitation at 2600 cm^{-1}. At this

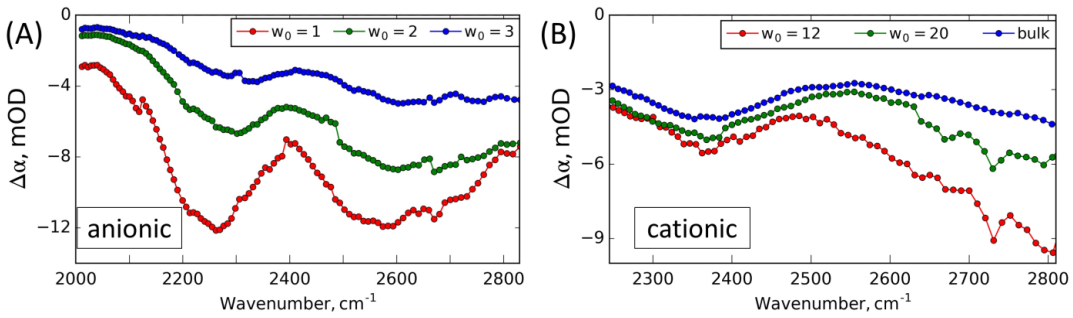

Fig. 2 Isotropic transient absorption spectra of hydrated protons (A) in anionic reverse micelles and (B) in cationic reverse micelles and in bulk aqueous solution. Excitation frequency ν_{ex}=2600 cm^{-1}, pump-probe delay time T_w=0.3 ps; the spectra are scaled for better comparison.

frequency we only excite OH-stretch vibrations in the core of the hydrated proton and not those of water molecules outside this core. In the frequency region of 2000-2800 cm^{-1} the transient spectra consist of a broad negative absorption change (for the details and the additional spectra see Experimental section and Figs. S1-S4 in the Supplementary Information).

The transient spectrum of the hydrated protons confined in anionic micelles shows two strong bands centered at ~2250 cm^{-1} and ~2600 cm^{-1}, which resemble the structure of the linear infrared spectrum of anionic micelles (Fig. 1B). For the hydrated protons in cationic micelles we observe a similar absorption spectrum. It can be also subdivided into two signatures: a band at ~2350 cm^{-1} and a slope at higher frequency (>2500 cm^{-1}), which is the low-frequency tail of an intense band at frequency >2800 cm^{-1}.

For hydrated protons in anionic reverse micelles there is a clear gradual change in the transient spectra with the increase of water content. The low-frequency band shifts from ~2250 cm^{-1} to ~2350 cm^{-1}, and the high-frequency band grows with respect to the low-frequency band. These spectral changes can result from different possible localization of the hydrated protons in the water pool.

In AOT-stabilized water nanodroplets protons can be solvated both in the core of the water pool and at the water-AOT interface. The sulfonate group of the AOT surfactant is negatively charged and thus a substantial fraction of the protons will be solvated in the vicinity of the sulfonate groups and/or substitute the sodium cations in the Stern layer.[30,31] For small micelles (w_0=1) all protons are inevitably located close to sulfonate groups of the AOT surfactant. With increasing micelle size the probability for protons to be hydrated in the center core of the nanodroplet increases.

We find that the transient spectrum of the larger anionic reverse micelles (w_0=3) can be constructed as a weighted sum of the transient spectrum of the smallest anionic reverse micelles with w_0=1 and that of the cationic reverse micelles of similar size (Fig. 3), reflecting that in large anionic micelles a fraction of the protons is close to, and strongly interacting with the AOT surfactants, while another fraction is located in the center core of the water nanodroplet. This result demonstrates that the spectroscopic response of hydrated protons in the center of the anionic reverse micelles resembles that of hydrated protons in cationic reverse micelles.

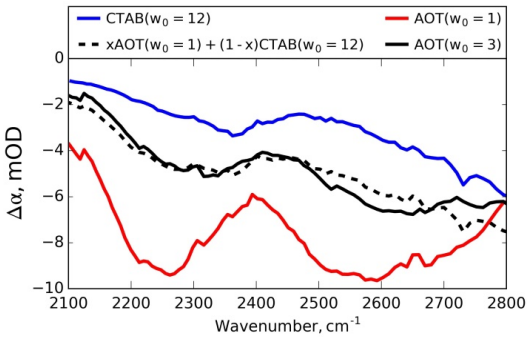

Fig. 3 Transient spectra of hydrated protons in small anionic reverse micelles (red line) and in cationic reverse micelles (blue line), the weighted sum of these two spectra (black dashed line) and the transient spectrum of hydrated protons in large anionic reverse micelles (black solid line).

The transient absorption spectrum of small AOT reverse micelles shows great similarity with the linear infrared spectra of concentrated solutions of ethanesulfonic acid (Fig. S5). From this similarity we conclude that the two bands at 2250 cm^{-1} and 2600 cm^{-1} can be assigned to a heteromolecular proton solvation complex. This complex can be seen as a contact ion pair [RSO_3^-–$H_3O^+(H_2O)_n$], in which the proton charge is shared by water molecules and an anionic sulfonate group. Raman[32] and NMR[33] experiments suggest that the basicity of alkanesulfonates in solution is similar to that of water. Hence, we expect that in the solvation complex [RSO_3^-–$H_3O^+(H_2O)_n$] the proton will be delocalized over the water molecules and the sulfonate group. The infrared spectra of concentrated ethanesulfonic acid solutions (Fig. S6) show that at a concentration ratio $EtSO_3H$:H_2O=1:1 about 85% of the acid is deprotonated, which indicates that the water molecules have a slightly stronger basicity than the ethanesulfonate anion. Thus, we expect that in [RSO_3^-–$H_3O^+(H_2O)_n$] complexes the proton charge is mostly delocalized over the water molecules.

In Fig. 4 we present the anisotropy of the transient absorption signal for anionic and cationic reverse micelles as a function of micelle size. For cationic reverse micelles the anisotropy at 2300 and 2600 cm^{-1} becomes lower with increasing micelle size.

This trend agrees with the facts that for bulk acid solutions the anisotropy value is lower (∼0.15 at 2600 cm^{-1} [29]), and that the core of the nanodroplet is expected to become increasingly bulk-like with increasing micelle size. For the anionic reverse micelles the anisotropy is low for the smallest reverse micelle with w_0=1, and increases with the size of the nanodroplet. This latter trend can be explained from the increasing contribution of the signal from the protons in the center core of the nanodroplet. As illustrated in Fig. 3, the signal of the anionic reversed micelles becomes increasingly similar to that of cationic reverse micelles with increase reverse micelle size.

The anisotropy represents the average relative orientation of the probed vibration with respect to the excited vibration. Here we see that the excitation at ∼2600 cm^{-1} results in different anisotropy values at 2300 and 2600 cm^{-1}, both in anionic and cationic reverse micelles, which implies that different vibrations with differently oriented transition dipole moments are being probed.

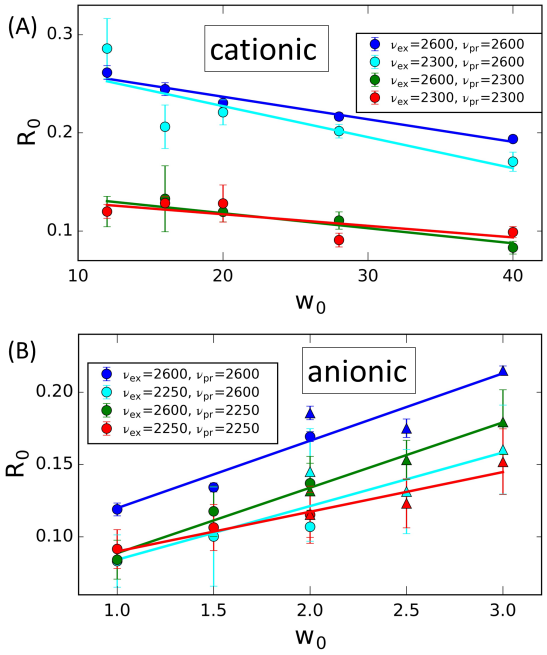

Fig. 4 Anisotropy of the low frequency band and the high frequency band following the excitation of each of them measured for cationic (A) and anionic (B) reverse micelles. The size of a CTAB cationic micelle with w_0=12 is approximately the same as that of an AOT anionic micelle with w_0=3. Anisotropy is obtained as $R=(\Delta\alpha_{\parallel}-\Delta\alpha_{\perp})/(\Delta\alpha_{\parallel}+2\Delta\alpha_{\perp})$, where $\Delta\alpha_{\parallel}$ and $\Delta\alpha_{\perp}$ are transient absorption signals measured in parallel and perpendicular polarization combination, respectively (see Supporting Information for the details). Straight lines are guides to the eye.

When pumping and probing at the same frequency, the initial anisotropy value R_0 represents the degeneracy of the vibration. For a non-degenerate vibration, the initial anisotropy value is 0.4. The fact that we observe lower initial anisotropy values indicates that the probed vibrations possess a certain degree of degeneracy.[29] The anisotropy is observed to be lower for low-frequency vibrations, indicating that the lower-frequency vibrations are more degenerate than the higher-frequency vibrations.

For the cationic reverse micelles the anisotropy is independent of the excitation frequency and is determined only by the degeneracy of the probed vibration. This is a consequence of the very weak absorption of the 2350 cm^{-1} band in the infrared spectrum. A pump pulse centered at 2300 cm^{-1} thus mostly excites higher frequency vibrations centered at 2800-3000 cm^{-1}. The relatively high anisotropy value of the transient absorption signal probed at 2600 cm^{-1} indicates that a large fraction of these high-frequency vibrations is quite well localized on a single OH-group.

For the anionic reverse micelles (Fig. 4B) we observe the lowest anisotropy for ν_{ex}=2250 cm^{-1} and ν_{pr}=2250 cm^{-1}, and the highest anisotropy for ν_{ex}=2600 cm^{-1} and ν_{pr}=2600 cm^{-1}. In this case the absorption bands of the low- and high-frequency vibration are of approximately equal strength, and the signal at each of the excitation/probing frequencies of 2250 and 2600 cm^{-1} will contain contributions of both bands. The highest anisotropy is thus observed when the less degenerate vibration with its absorption band centered at 2600 cm^{-1} is both excited and probed.

The interpretation of the transient spectra of protons in cationic and anionic reverse micelles is aided by the comparison with infrared photodisocciation (IRPD) spectra of small hydrated proton clusters at low temperatures. This comparison should be carried out with some care, as the vibrational frequencies of hydrated protons in liquid water are subject to fast fluctuations of significant amplitude that result in a strong broadening of the vibrational bands compared to what is observed for small clusters at low temperatures. However, it has been observed that the vibrational spectra of hydrated proton clusters show a distinct structure that strongly depends on the hydrogen-bond structure of the first hydration shell.[17] Hence, if the liquid phase spectrum shows characteristic features that agree with the observations for particular hydrated proton clusters, it appears quite likely that the first hydration shell in the liquid phase possesses a similar structure as those clusters.

IRPD experiments on protonated water clusters showed that in a perfectly symmetric $D_3O^+(D_2O)_3$ structure, the absorption bands of the three OD-stretch vibrations of the central D_3O^+ moiety overlap, constituting a single broad absorption band.[17] Addition of a hydrogen-bond accepting molecule to one of the D_2O molecules of the cluster makes this molecule a stronger hydrogen bond acceptor, thus distorting the C_{3v} symmetrical structure and resulting in a split of the single broad OD-stretch band of D_3O^+.[16,17,34,35]

A similar split of the OH absorption band of the H_3O^+ core is observed if one of the OH groups is more weakly hydrogen bonded than the other two OH groups. The limiting case of such an asymmetric structure is the protonated water trimer H_2O–H_3O^+–H_2O, in which two OH-groups of the H_3O^+ core are hydrogen bonded to H_2O molecules and one OH-group is non bonded. Such $H_7O_3^+$ structures were observed for hydrated super acids in crystals and in nonpolar solvents.[36–39]

These properties of asymmetric hydrated proton structures have been studied in detail in IRPD experiments on the protonated water trimer $(H_3O^+(H_2O)_2)$,[18,40] pentamer $(H_3O^+(H_2O)_4)$,[13,35] and hexamer $(H_3O^+(H_2O)_5)$[16]. For the pentamer $H_3O^+(H_2O)_4$ bands at ∼2600 cm^{-1} and ∼2800 cm^{-1}

where the band at 2600 cm^{-1} is assigned to the near-degenerate symmetric and antisymmetric vibrations of the two relatively strongly hydrogen bonded OH-groups of H_3O^+, and the band at 2800 cm^{-1} is assigned to the stretch vibration of the less strongly hydrogen-bonded OH group.[13] Furthermore, it is observed that with increasing difference in hydrogen-bond strengths of the three OH groups of the central H_3O^+ ion, the band at 2600 cm^{-1} shifts to lower frequencies (∼2400 cm^{-1} for $H_3O^+(H_2O)_5$ and 1900-2300 cm^{-1} for the extremely asymmetric $H_3O^+(H_2O)_2$), and the band at 2800 cm^{-1} shifts to higher frequencies (∼3000 cm^{-1} for $H_3O^+(H_2O)_5$ and ∼3600 cm^{-1} for the free OH-group of $H_3O^+(H_2O)_2$).

The spectra of acid water in anionic and cationic micelles show similar spectral characteristics as the clusters. The spectra of protons in AOT reverse micelles contain two bands at 2250 cm^{-1} and 2600 cm^{-1}. The band at 2250 cm^{-1}, that the anisotropy measurements show to represent a more degenerate vibration, matches well with the bands at 1900-2600 cm^{-1} observed in IRPD experiments. Therefore, we assign this band to the degenerate symmetric and antisymmetric OH-stretch vibrations of two strongly hydrogen-bonded OH groups of the central H_3O^+ ion of the proton hydration structure. The band at 2600 cm^{-1}, that the anisotropy measurements show to represent a less degenerate vibration, can be assigned to the stretch vibration of the third, less strongly hydrogen-bonded OH group of the central H_3O^+ ion of the proton hydration structure.

For AOT micelles with low water content (low w_0), the asymmetry in the proton hydration structures likely results from the interaction of the central H_3O^+ ion with sulfonate (SO_3^-) groups. In several theoretical calculations it was shown that the most favorable hydration structure of sulfonic acids is formed by the [RSO_3^-–$H_3O^+(H_2O)_2$] motif.[41–44] In this complex, the sulfonate group is a weaker hydrogen bond acceptor than the two H_2O molecules. Hence, the band at 2600 cm^{-1} can be assigned to the OH groups that is more weakly hydrogen bonded to sulfonate, and the band at 2250 cm^{-1} can be assigned to the two other OH-groups that are more strongly hydrogen bonded to water molecules. The degeneracy of the stretch vibrations of the strongly hydrogen-bonded OH groups results in a low anisotropy value of ∼0.1, in agreement with our observations for the low-frequency band. Due to the relatively high concentration of AOT molecules, most of which interact with sodium cations, the two water molecules accepting the two stronger hydrogen bonds from H_3O^+ most likely donate hydrogen bonds to sulfonate groups of other AOT molecules.

The proton hydration structures in cationic reverse micelles are also largely asymmetric, which is demonstrated by the relatively high anisotropy value of ∼0.25 observed at 2600 cm^{-1}. This high anisotropy value indicates that the absorption at frequencies >2500cm^{-1} is dominated by proton-hydration structures for which one of the three OH groups of the H_3O^+ core is more weakly hydrogen bonded than the other two OH groups.

We propose that the weak absorption band at 2350 cm^{-1} observed for acid cationic reverse micelles and acid bulk water originates from a (near-)symmetric [$H_3O^+(H_2O)_3$] complex. Replacing the SO_3^- group in the asymmetric [RSO_3^-–$H_3O^+(H_2O)_2$] complex by H_2O is thus proposed to lead to the merging of the two bands at 2250 cm^{-1} and 2600 cm^{-1} into a single band at 2350 cm^{-1}. This interpretation is supported by the observation that the anisotropy of the transient absorption signal at 2350 cm^{-1} has a value of ∼0.1 (Fig. 4A), which is the value that would result from the complete randomization of a vibrational excitation in a plane. Hence, an anisotropy value of ∼0.1 corresponds well to the case of 3 near-degenate OH vibrations of a planar, symmetrically hydrogen-bonded H_3O^+ core.

It is clear from the linear infrared spectrum of acid cationic reverse micelles and acid bulk water that the band at 2350 cm^{-1} is relatively weak, which implies that only a small fraction of the proton hydration structures will be symmetric. Most of the proton-hydration structures in acid cationic reverse micelles and acid bulk water will thus be asymmetric, as illustrated by the strong absorption near 2800 cm^{-1}. The large abundance of asymmetric proton hydration structures can be explained from the fact that in the studied cationic reverse micelles and bulk water the proton hydration structures are surrounded by a large number of water molecules and counterions (second and third solvation shells), that show a large variation in composition and hydrogen-bond structure, thus inducing a large variation in the strengths of the hydrogen bonds of the three OH groups of the central H_3O^+ core.

Conclusions

In summary, we investigated the OH-stretch absorption spectrum of hydrated protons in cationic and anionic reverse micelles with linear infrared absorption spectroscopy and femtosecond transient absorption spectroscopy. The vibrational spectrum of hydrated protons in small anionic AOT reverse micelles shows two distinct bands at 2250 and 2600 cm^{-1}. These two bands correspond to two different vibrations of the same proton hydration structure. The anisotropy of the bands shows that the low-frequency vibration is more degenerate than the high frequency vibration. Comparing our results with the results of studies of small hydrated proton clusters and studies of hydrated sulfonic acids, we assign the two bands to OH stretch vibrations of the H_3O^+ core of a [RSO_3^-–$H_3O^+(H_2O)_2$] complex. The band at 2600 cm^{-1} is assigned to the stretch vibration of the OH group that is more weakly hydrogen bonded to sulfonate, and the band at band at 2250 cm^{-1} is assigned to the two other OH-groups that are more strongly hydrogen bonded to water molecules.

For acid cationic reverse micelles and acid bulk water we observe a weak band at 2350 cm^{-1}. We propose that this band corresponds to a symmetric [$H_3O^+(H_2O)_3$]. Hence, replacing the SO_3^- group by H_2O leads to the merging of the two bands at 2250 cm^{-1} and 2600 cm^{-1} into a single band at 2350 cm^{-1}. The symmetric complex constitutes only a minor fraction of the proton-hydration complexes in acid cationic reverse micelles and acid bulk water. Most of the complexes are asymmetric proton-hydration structures for which one of the three OH groups of the H_3O^+ core is more weakly hydrogen bonded than the other two OH groups.

Conflicts of interest

There are no conflicts to declare.

Acknowledgements

This work is part of the research program of the Netherlands Organization for Scientific Research (NWO) and was performed at the research institute AMOLF. This project has received funding from the European Research Council (ERC) under the European Union's Horizon 2020 research and innovation program (grant agreement No 694386). The authors thank Hinco Schoenmaker for the experimental support and Alexander Korotkevich for the discussion.

Notes and references

1 N. Agmon, *Chemical Physics Letters*, 1995, **244**, 456–462.
2 O. Markovitch, H. Chen, S. Izvekov, F. Paesani, G. A. Voth and N. Agmon, *The Journal of Physical Chemistry B*, 2008, **112**, 9456–9466.
3 C. Knight and G. A. Voth, *Accounts of chemical research*, 2012, **45**, 101–109.
4 J. Xu, Y. Zhang and G. A. Voth, *The journal of physical chemistry letters*, 2011, **2**, 81–86.
5 D. Decka, G. Schwaab and M. Havenith, *Physical Chemistry Chemical Physics*, 2015, **17**, 11898–11907.
6 M. Śmiechowski and J. Stangret, *The Journal of chemical physics*, 2006, **125**, 204508.
7 F. Dahms, B. P. Fingerhut, E. T. Nibbering, E. Pines and T. Elsaesser, *Science*, 2017, **357**, 491–495.
8 J. A. Fournier, W. B. Carpenter, N. H. Lewis and A. Tokmakoff, *Nature chemistry*, 2018, **10**, 932–937.
9 A. Kundu, F. Dahms, B. P. Fingerhut, E. T. Nibbering, E. Pines and T. Elsaesser, *The journal of physical chemistry letters*, 2019, **10**, 2287–2294.
10 E. S. Stoyanov, I. V. Stoyanova and C. A. Reed, *Chemical Science*, 2011, **2**, 462–472.
11 C. A. Reed, *Accounts of chemical research*, 2013, **46**, 2567–2575.
12 W. Kulig and N. Agmon, *Journal of Physical Chemistry B*, 2014, **118**, 278–286.
13 W. Kulig and N. Agmon, *Physical Chemistry Chemical Physics*, 2014, **16**, 4933–4941.
14 R. Biswas, W. Carpenter, J. A. Fournier, G. A. Voth and A. Tokmakoff, *The Journal of chemical physics*, 2017, **146**, 154507.
15 J. Kim, U. W. Schmitt, J. A. Gruetzmacher, G. A. Voth and N. E. Scherer, *The Journal of chemical physics*, 2002, **116**, 737–746.
16 N. Heine, M. R. Fagiani, M. Rossi, T. Wende, G. Berden, V. Blum and K. R. Asmis, *Journal of the American Chemical Society*, 2013, **135**, 8266–8273.
17 C. T. Wolke, J. A. Fournier, L. C. Dzugan, M. R. Fagiani, T. T. Odbadrakh, H. Knorke, K. D. Jordan, A. B. McCoy, K. R. Asmis and M. A. Johnson, *Science*, 2016, **354**, 1131–1135.
18 N. R. Samala and N. Agmon, *Chemical Physics*, 2018, **514**, 164–175.
19 X. Zhao, R. P. Bagwe and W. Tan, *Advanced Materials*, 2004, **16**, 173–176.
20 M. Jafelicci Jr, M. R. Davolos, F. J. dos Santos and S. J. de Andrade, *Journal of non-crystalline solids*, 1999, **247**, 98–102.
21 Y.-G. Han, T. Kusunose and T. Sekino, *Synthetic Metals*, 2009, **159**, 123–131.
22 M. D. Fayer and N. E. Levinger, *Annual Review of Analytical Chemistry*, 2010, **3**, 89–107.
23 D. Munoz-Santiburcio and D. Marx, *Chemical science*, 2017, **8**, 3444–3452.
24 F. Dahms, R. Costard, E. Pines, B. P. Fingerhut, E. T. Nibbering and T. Elsaesser, *Angewandte Chemie International Edition*, 2016, **55**, 10600–10605.
25 N. Ottosson, L. Liu and H. Bakker, *The Journal of Physical Chemistry B*, 2016, **120**, 7154–7163.
26 O. O. Sofronov and H. J. Bakker, *The Journal of Physical Chemistry B*, 2019, **123**, 6222–6228.
27 O. O. Sofronov and H. J. Bakker, *The Journal of Physical Chemistry B*, 2018, **122**, 10005–10013.
28 W. B. Carpenter, J. A. Fournier, N. H. Lewis and A. Tokmakoff, *The Journal of Physical Chemistry B*, 2018, **122**, 2792–2802.
29 O. O. Sofronov and H. J. Bakker, *ACS Central Science*, 2020, **6**, 1150—-1158.
30 H. R. Rabie and J. H. Vera, *The Journal of Physical Chemistry B*, 1997, **101**, 10295–10302.
31 P. Mukherjee, S. Gupta, S. Rafiq, R. Yadav, V. K. Jain, J. Raval and P. Sen, *Langmuir*, 2016, **32**, 1693–1699.
32 A. K. Covington and R. Thompson, *Journal of Solution Chemistry*, 1974, **3**, 603–617.
33 A. Telfah, G. Majer, K. Kreuer, M. Schuster and J. Maier, *Solid State Ionics*, 2010, **181**, 461–465.
34 J. A. Fournier, C. T. Wolke, M. A. Johnson, T. T. Odbadrakh, K. D. Jordan, S. M. Kathmann and S. S. Xantheas, *Journal of Physical Chemistry A*, 2015, **119**, 9425–9440.
35 M. R. Fagiani, H. Knorke, T. K. Esser, N. Heine, C. T. Wolke, S. Gewinner, W. Schöllkopf, M.-P. Gaigeot, R. Spezia, M. A. Johnson *et al.*, *Physical Chemistry Chemical Physics*, 2016, **18**, 26743–26754.
36 E. S. Stoyanov, I. V. Stoyanova, F. S. Tham and C. A. Reed, *Journal of the American Chemical Society*, 2008, **130**, 12128–12138.
37 E. S. Stoyanov, *Journal of the Chemical Society, Faraday Transactions*, 1997, **93**, 4165–4175.
38 E. S. Stoyanov, K.-C. Kim and C. A. Reed, *The Journal of Physical Chemistry A*, 2004, **108**, 9310–9315.
39 E. S. Stoyanov, K.-C. Kim and C. A. Reed, *Journal of the American Chemical Society*, 2006, **128**, 1948–1958.
40 C. H. Duong, O. Gorlova, N. Yang, P. J. Kelleher, M. A. Johnson, A. B. McCoy, Q. Yu and J. M. Bowman, *The journal of physical chemistry letters*, 2017, **8**, 3782–3789.
41 T. Ishimoto, T. Ogura and M. Koyama, *Computational and Theoretical Chemistry*, 2011, **975**, 92–98.
42 S. Paddison, *Journal of New Materials for Electrochemical Systems*, 2001, **4**, 197–208.
43 D. Kurniawan, S. Morita and K. Kitagawa, *Computational and Theoretical Chemistry*, 2012, **982**, 30–33.
44 T. Shimoaka, C. Wakai, T. Sakabe, S. Yamazaki and T. Hasegawa, *Physical Chemistry Chemical Physics*, 2015, **17**, 8843–8849.